

Contribution from the Department of Inorganic Chemistry,
Indian Association for the Cultivation of Science, Calcutta 700 032, India

A Family of Mononuclear Manganese(IV) Complexes: An $Mn^{IV}O_4N_2$ Sphere Assembled via Phenolate–Imine–Carboxylate Coordination

Swapan Kumar Chandra, Partha Basu, Debashis Ray, Samudranil Pal, and Animesh Chakravorty*

Received September 29, 1989

Manganese(IV) complexes (MnL_2) of tridentate Schiff bases (H_2L) carrying a carboxylate function are described. The specific ligands H_2als , H_2ans , and H_2ann are derived from salicylaldehyde and β -alanine, salicylaldehyde and anthranilic acid, and 2-hydroxynaphthaldehyde and anthranilic acid, respectively. The reaction of H_2L with manganese(III) acetate dihydrate affords $KMnL_2 \cdot H_2O$, which upon chemical ($S_2O_8^{2-}$, Ag^+) or electrochemical (0.75 V vs SCE) oxidation in methanol affords MnL_2 in high yields. The structure of $Mn(als)_2$ has been determined ($R = 0.0438$ and $R_w = 0.0581$) by X-ray crystallography: space group $C2/c$; $Z = 4$; $a = 17.314$ (5) Å, $b = 7.884$ (3) Å, $c = 13.104$ (3) Å, $\beta = 91.86$ (2)°, $V = 1787.8$ (9) Å³. In the octahedral MnO_4N_2 coordination sphere each ligand acts as a meridional ONO donor utilizing phenolic ($Mn-O = 1.860$ (2) Å) and carboxylate oxygen ($Mn-O = 1.907$ (2) Å) atoms and the azomethine nitrogen ($Mn-N = 2.004$ (3) Å) atom. Each salicylaldehyde fragment is planar, but the manganese(IV) atom is displaced by 0.64 Å from it. The β -alanine residue forms a chelate ring with a boatlike appearance, the dimethylene fragment being in gauche configuration. The magnetic moments (3.96–4.13 μ_B) of the MnL_2 complexes correspond to the d^3 configuration. Their EPR spectra (77 K) consist of strong and weak signals near $g = 4$ and $g = 2$ (⁵⁵Mn hyperfine structure), respectively. There is strong axial distortion associated with a small rhombic component. This is rationalized in terms of elongation of the MnO_4N_2 coordination sphere along the MnN_2 axis. Analogy is drawn between MnL_2 and the manganese(IV) center of photosystem II. The $Mn^{IV}L_2$ – $Mn^{III}L_2^-$ couple has a reduction potential of ~ 0.5 V vs SCE (cyclic voltammetry). A second couple, presumably $Mn^{III}L_2^-$ – $Mn^{II}L_2^{2-}$, occurs near -0.2 V vs SCE, but the manganese(II) species is unstable. The effect of carboxylate coordination on the reduction potentials is noted. The role of $X-O^-$ ($X =$ monovalent group, possibly with additional coordinating atoms for chelation) ligands in manganese(IV) binding is stressed. The present ligands belong to this class.

Introduction

Manganese(IV) is an enigmatic oxidation state: it is uncommon in coordination chemistry and yet it is believed to be active in one of the most common reactions of nature namely photosynthetic oxygen evolution.¹ The number of authentic mononuclear manganese(IV) complexes that have been isolated in the pure state is indeed limited.^{2–12} We find this surprising for a simple reason.

Table I. Magnetic Moments, Molar Conductivity Values, and Electronic Spectral Data for $KMnL_2 \cdot H_2O$

compd	μ_{eff}^a , μ_B	Λ_M^b , $\Omega^{-1} \text{ cm}^2 \text{ M}^{-1}$	UV-vis data: ^b λ_{max} , nm (ϵ , $\text{M}^{-1} \text{ cm}^{-1}$)
$KMn(als)_2 \cdot H_2O$	4.95	75	1020 (65), 600 ^c (210), 375 (4700), 280 ^c (15 700)
$KMn(ans)_2 \cdot H_2O$	4.94	73	975 (54), 640 (330), 400 (9100), 290 ^c (26 600)
$KMn(ann)_2 \cdot H_2O$	4.96	70	980 ^c (94), 630 ^c (450), 430 (16 300), 330 (25 600)

^aIn the solid state at 298 K. ^bThe solvent is methanol. ^cShoulder.

The oxidation states that characterize major terrestrial minerals (ores) of 3d elements are invariably stable enough to be sustained in a variety of synthetic coordination compounds. Examples are titanium(IV), vanadium(V), chromium(III), iron(III), etc. Manganese(IV) should find a natural place in this sequence, since the most important mineral of manganese in pyrolusite, $Mn^{IV}O_2$. We believe that the paucity of manganese(IV) complexes is more due to lack of search than due to any particular instability. Our endeavor in manganese(IV) chemistry is set in this background.

A few years ago we reported the $Mn^{IV}S_3O_3$ coordination sphere in tris thiohydroxamates.⁴ For binding metal ions carrying large positive charges, it is a good strategy^{13,14} to employ strongly electronegative donors in their anionic form e.g., O^{2-} or, when electron demand is less stringent, $X-O^-$ ($X =$ monovalent group possibly with additional coordinating atoms for chelation). The $X-O^-$ strategy appears to work quite well for manganese(IV): it

- (1) (a) Dismukes, G. C. *Photochem. Photobiol.* **1986**, *43*, 99–115. (b) DePaula, J. C.; Brudvig, G. W. *J. Am. Chem. Soc.* **1985**, *107*, 2643–2648. (c) Livorness, J.; Smith, T. D. *Struct. Bonding (Berlin)* **1982**, *48*, 1–44. (d) Kirby, J. A.; Robertson, A. S.; Smith, J. P.; Thompson, A. C.; Cooper, S. R.; Klein, M. P. *J. Am. Chem. Soc.* **1981**, *103*, 5529–5536. (e) Sauer, K. *Acc. Chem. Res.* **1980**, *13*, 249–256. (f) Hansson, Ö.; Aasa, R.; Vänngård, T. *Biophys. J.* **1987**, *51*, 825–832.
- (2) Cotton, F. A.; Wilkinson, G. *Advanced Inorganic Chemistry*, 4th ed.; Wiley: New York, 1980; pp 744–746.
- (3) Dithiocarbamates: (a) Deplano, P.; Trogu, E. F.; Bigoli, F.; Pellingheli, M. A. *J. Chem. Soc., Dalton Trans.* **1987**, 2407–2410. (b) Brown, K. L.; Golding, R. M.; Healy, P. C.; Jessop, K. J.; Tennant, W. C. *Aust. J. Chem.* **1974**, *27*, 2075–2081. (c) Hendrickson, A. R.; Martin, R. L.; Rohde, N. M. *Inorg. Chem.* **1974**, *13*, 1933–1939. (d) Saleh, R. Y.; Straub, D. K. *Inorg. Chem.* **1974**, *13*, 3017–3019.
- (4) Thiohydroxamates: Pal, S.; Ghosh, P.; Chakravorty, A. *Inorg. Chem.* **1985**, *24*, 3704–3706.
- (5) Phenoxides and alkoxide: (a) Lynch, M. W.; Hendrickson, D. N.; Fitzgerald, B. J.; Pierpont, C. G. *J. Am. Chem. Soc.* **1984**, *106*, 2041–2049. (b) Hartman, J. R.; Foxman, B. M.; Cooper, S. R. *Inorg. Chem.* **1984**, *23*, 1381–1387. (c) Chun, D.-H.; Sawyer, D. T.; Schaeffer, W. P.; Simmons, C. J. *Inorg. Chem.* **1983**, *22*, 752–758. (d) Richens, D. T.; Sawyer, D. T. *J. Am. Chem. Soc.* **1979**, *101*, 3681–3683.
- (6) Schiff bases: (a) Kessissoglou, D. P.; Li, X.; Butler, W. M.; Pecoraro, V. L. *Inorg. Chem.* **1987**, *26*, 2487–2492. (b) Tirant, M.; Smith, T. D. *Inorg. Chim. Acta* **1986**, *121*, 5–11. (c) Fujiwara, M.; Matsushita, T.; Shono, T. *Polyhedron* **1985**, *4*, 1895–1900. (d) Okawa, H.; Nakamura, M.; Kida, S. *Bull. Chem. Soc. Jpn.* **1982**, *55*, 466–470.
- (7) Carboxylate: Pavacic, P. S.; Huffman, J. C.; Christou, G. *J. Chem. Soc., Chem. Commun.* **1986**, 43–44.
- (8) Amides: (a) Chandra, S. K.; Choudhury, S. B.; Ray, D.; Chakravorty, A. *J. Chem. Soc., Chem. Commun.*, in press. (b) Koikawa, M.; Okawa, H.; Kida, S. *J. Chem. Soc., Dalton Trans.* **1988**, 641–645.
- (9) Porphinates: (a) Camenzind, M. J.; Hollander, F. J.; Hill, C. L. *Inorg. Chem.* **1983**, *22*, 3776–3784. (b) Smegal, J. A.; Hill, C. L. *J. Am. Chem. Soc.* **1983**, *105*, 2920–2922. (c) Camenzind, M. J.; Hollander, F. J.; Hill, C. L. *Inorg. Chem.* **1982**, *21*, 4301–4308.
- (10) Organometallics: (a) Howard, C. G.; Girolami, G. S.; Wilkinson, G.; Thornton-Pett, M.; Hursthouse, M. B. *J. Chem. Soc., Chem. Commun.* **1983**, 1163–1164. (b) Bower, B. K.; Tennent, H. G. *J. Am. Chem. Soc.* **1972**, *94*, 2513–2514.
- (11) Halogeno complexes: (a) Bukovec, P.; Hoppe, R. *J. Fluorine Chem.* **1983**, *23*, 579–587. (b) Moews, P. *Inorg. Chem.* **1966**, *5*, 5–8.

- (12) In this article we are concerned with the mononuclear manganese(IV) complexes. Examples of multinuclear complexes containing manganese(IV) are also rare: (a) Wiegand, K.; Bossek, U.; Nuber, B.; Weiss, J.; Bonvoisin, J.; Corbella, M.; Vitols, S. E.; Girerd, J. J. *J. Am. Chem. Soc.* **1988**, *110*, 7398–7411. (b) Matsushita, T.; Spencer, L.; Sawyer, D. T. *Inorg. Chem.* **1988**, *27*, 1167–1173. (c) Hagen, K. S.; Armstrong, W. H.; Hope, H. *Inorg. Chem.* **1988**, *27*, 967–969. (d) Collins, M. A.; Hodgson, D. J.; Michelsen, K.; Towle, D. K. *J. Chem. Soc., Chem. Commun.* **1987**, 1659–1660. (e) Stebler, M.; Ludi, A.; Bürgi, H.-B. *Inorg. Chem.* **1986**, *25*, 4743–4750. (f) Plaskin, P. M.; Stouffer, R. C.; Mathew, M.; Palenik, G. J. *J. Am. Chem. Soc.* **1972**, *94*, 2121–2122. (g) Smegal, J. A.; Schardt, B. C.; Hill, C. L. *J. Am. Chem. Soc.* **1983**, *105*, 3510–3515. (h) Schardt, B. C.; Hollander, F. J.; Hill, C. L. *J. Am. Chem. Soc.* **1982**, *104*, 3964–3972.
- (13) Nag, K.; Chakravorty, A. *Coord. Chem. Rev.* **1980**, *33*, 87–147.
- (14) Nyholm, R. S.; Tobe, M. L. *Adv. Inorg. Chem. Radiochem.* **1963**, *5*, 1–40.

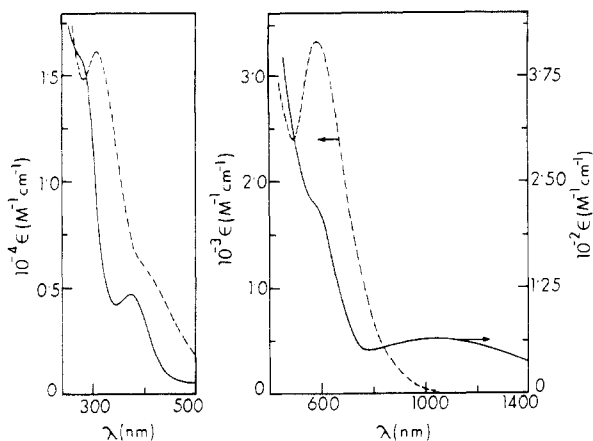


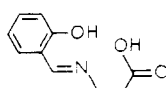
Figure 1. Electronic spectra of $\text{KMn(als)}_2 \cdot \text{H}_2\text{O}$ (—) and Mn(als)_2 (---) in methanol.

encompasses thiohydroxamates,⁴ hydroxyl-rich ligands,^{6a,15} and some other donors employed.⁵⁻⁸

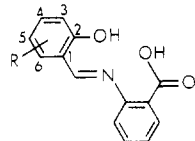
Herein we describe a group of neutral mononuclear manganese(IV) bis chelates coordinated to tridentate dianionic ONO Schiff bases derived from hydroxyaldehydes and amino acids. The complexes along with their manganese(III) congeners have been examined by using spectral, magnetic, and electrochemical techniques. The structure of one manganese(IV) complex has been determined by X-ray crystallography. Coordination occurs at phenolic and carboxylate oxygen and imine nitrogen. The coordination environment and EPR spectra of the complexes partially mimic those of the water-oxidation complex of photosystem II.

Results

A. Ligands and Manganese(III) Precursors. The ligands H_2als (1), H_2ans (2a) and H_2ann (2b) (general abbreviation H_2L) ob-



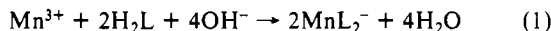
1 $\text{H}_2\text{L} = \text{H}_2\text{als}$



2a R = H; $\text{H}_2\text{L} = \text{H}_2\text{ans}$

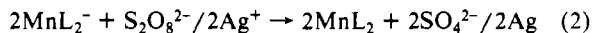
2b R = 5,6-benzo; $\text{H}_2\text{L} = \text{H}_2\text{ann}$

tained as yellow to orange solids by Schiff base condensation were reacted with manganese(III) acetate dihydrate in alkaline (KOH) methanol to afford monoanionic bis manganese(III) chelates (eq 1). These were isolated in high yields as hydrated potassium(I)



salts. Characterization data for the complexes are given in Table I. Their magnetic moments confirm to the usual high-spin d^4 configuration. As is usual for high-spin manganese(III) complexes, these are EPR-silent even at 77 K. The absorption spectrum of $\text{KMn(als)}_2 \cdot \text{H}_2\text{O}$ is illustrated in Figure 1. Solution electrical conductivities are slightly lower than 1:1 electrolytic values possibly due to ion association.

B. Synthesis of Tetravalent Complexes. The manganese(III) complexes are stable in air. Oxidation to the manganese(IV) species MnL_2 can be achieved chemically in excellent yield in aqueous methanol by using $\text{S}_2\text{O}_8^{2-}$ or Ag^+ as oxidant (eq 2). Both



oxidants are convenient in the case of Mn(als)_2 . The Mn(ans)_2 and Mn(ann)_2 complexes are very poorly soluble, and here $\text{S}_2\text{O}_8^{2-}$ is preferable to avoid contamination by metallic silver. Synthesis

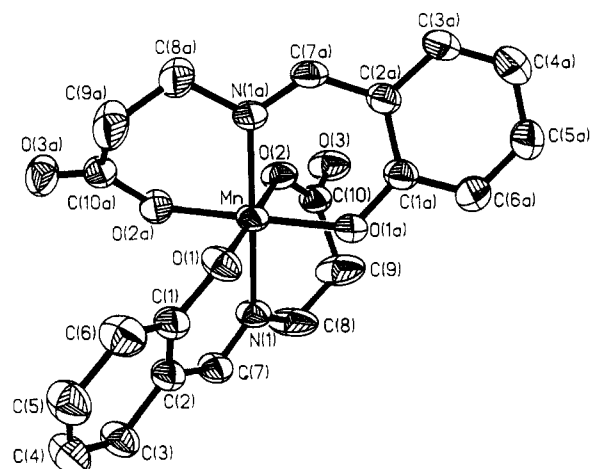


Figure 2. ORTEP plot and labeling scheme for Mn(als)_2 . All atoms are represented by their 50% probability ellipsoids.

Table II. Selected Bond Distances (Å) and Angles (deg) and Their Estimated Standard Deviations for Mn(als)_2 ^a

Distances			
Mn-N(1)	2.004 (3)	O(2)-C(10)	1.298 (4)
Mn-O(1)	1.860 (2)	O(3)-C(10)	1.211 (4)
Mn-O(2)	1.907 (2)	C(9)-C(10)	1.509 (5)
N(1)-C(7)	1.287 (4)	C(9)-C(8)	1.432 (5)
N(1)-C(8)	1.482 (4)	C(2)-C(7)	1.437 (5)
O(1)-C(1)	1.328 (3)		
Angles			
N(1)-Mn-O(1)	90.0 (1)	Mn-N(1)-C(8)	121.4 (2)
N(1)-Mn-O(2)	90.0 (1)	Mn-N(1)-Cn7	122.7 (2)
N(1)-Mn-O(2A)	88.9 (1)	Mn-O(2)-C(10)	131.0 (2)
N(1)-Mn-O(1A)	91.1 (1)	Mn-O(1)-C(1)	125.3 (2)
O(1)-Mn-N(1A)	91.1 (1)	O(1)-C(1)-C(2)	122.2 (3)
O(1)-Mn-O(1A)	89.7 (1)	C(1)-C(2)-C(7)	121.7 (3)
O(1)-Mn-O(2A)	91.2 (1)	N(1)-C(7)-C(2)	125.8 (3)
O(2)-Mn-N(1A)	88.9 (1)	N(1)-C(8)-C(9)	116.8 (3)
O(2)-Mn-O(1A)	91.2 (1)	C(8)-C(9)-C(10)	117.7 (3)
O(2)-Mn-O(2A)	87.8 (1)	O(2)-C(10)-C(9)	116.2 (3)
O(2)-Mn-O(1)	179.0 (1)	O(2)-C(10)-O(3)	122.5 (3)
N(1)-Mn-N(1A)	178.5 (2)	C(9)-C(10)-O(3)	121.3 (3)

^aNumbers in parentheses are estimated standard deviations in the least significant digits.

of the complexes is also achievable by anodic oxidation at 0.75 V vs SCE in dry methanol. This technique is particularly suited for Mn(ans)_2 and Mn(ann)_2 , which spontaneously precipitate from the electrolyzed solution.

Among the three complexes only Mn(als)_2 is soluble in methanol and dichloromethane, giving green nonconducting solutions. All MnL_2 species are solubilized by dimethylformamide and dimethyl sulfoxide but with decomposition and loss of color. Quantitative solution studies could therefore be performed only in the case of Mn(als)_2 in dichloromethane/methanol. The characteristic electronic spectrum of Mn(als)_2 in methanol is displayed in Figure 1. The transitions at 580, 410, and 310 nm have extinction coefficients of 3350, 5700, and 16 100 $\text{M}^{-1} \text{cm}^{-1}$, respectively. The corresponding band positions of other compounds (too insoluble for quantitative intensity studies) in dichloromethane are as follows: Mn(ans)_2 , 580, 450, 360, and 300 nm; Mn(ann)_2 , 660, 470, 370, and 335 nm. The bands in the range 400–700 nm are likely to be of charge-transfer origin. Ligand field bands were not observable in MnL_2 .

C. Crystal and Molecular Structure of Mn(als)_2 . The lattice consists of discrete Mn(als)_2 molecules. There are no significant intermolecular bonding contacts. An ORTEP drawing of the complex with atom-labeling scheme is shown in Figure 2. Selected bond parameters are listed in Table II.

The two ligands are related by a crystallographically imposed 2-fold axis of symmetry passing through Mn and between O(1) and O(1A) as well as between O(2) and O(2A). Each ligand acts

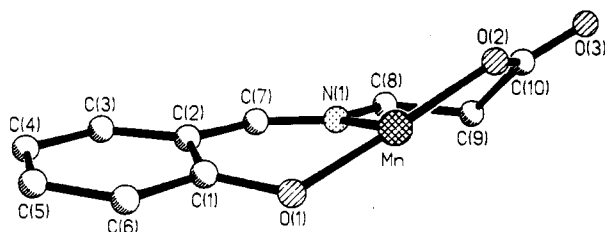


Figure 3. View of the chelate rings in $\text{Mn}(\text{als})_2$.

Table III. Magnetic Moments (298 K) and EPR Data (77 K) for MnL_2

compd	μ_{eff}^a , μ_B	g values ^b
$\text{Mn}(\text{als})_2$	3.96	3.86, ^{c,d} 2.02 ^{d,e}
$\text{Mn}(\text{ans})_2$	4.06	3.82, ^{c,f} 1.90 ^f
$\text{Mn}(\text{ann})_2$	4.13	3.95, ^{c,f} 1.92 ^f

^a In solid state. ^b Calculated by using DPPH ($g = 2.0037$) as calibrant. ^c Average value of turnover and crossover points. ^d In dichloromethane-toluene (1:1) glass. ^e The $g = 2.02$ signal splits into six components with A in the range 65–90 G with an average of 77 G. ^f Powder.

as a meridional ONO donor. In terms of angles within the coordination sphere, MnO_4N_2 is very close to an ideal octahedron. The ranges of cis and trans angles at the metal center are 87.8 (1)–91.2 (1) and 178.5 (2)–179.0 (1)°, respectively. The MnO_4 fragment is perfectly planar within experimental error; the planarity of Mn, O(1), O(2), N(1), and N(1A) (and hence of Mn, O(1A), O(2A), N(1), and N(1A)) is also exceedingly good: the maximum deviation from the mean plane is 0.01 Å (Mn). The three planes are orthogonal to one another, the average dihedral angle being 90.0 (1)°.

The salicylaldehyde fragment, C(1)–C(7), O(1), and N(1), constitutes a satisfactory plane with a mean deviation of 0.03 Å from it. However, the Mn atom does not lie on this plane—it is 0.64 Å above it. Thus the phenol-imine chelate ring is folded along the O(1), N(1) line—the fold angle being 27.7 (1)°. The observed folding is akin to the “step”-forming distortion in chelates of salicylaldehydes.¹⁶ The β -alanine chelate has a boatlike appearance with the dimethylene fragment in gauche configuration. The N(1), C(8), C(10), O(3), and O(2) atoms constitute a satisfactory plane (mean deviation 0.05 Å) from which the C(9) and Mn atoms are deflected by 0.62 and 0.39 Å, respectively. A perspective view of chelate ring conformation is depicted in Figure 3.

Among the few^{17,18} structurally characterized mononuclear manganese(IV) complexes only one⁷ involves carboxylate oxygen (O_c) coordination and one^{6a} has salicylaldehyde phenolic oxygen (O_p) and azomethine nitrogen (N_m) coordination: the average distances are $\text{Mn}-\text{O}_c = 1.876(5)$ Å, $\text{Mn}-\text{O}_p = 1.906(7)$ Å, and $\text{Mn}-\text{N}_m = 2.005(7)$ Å. In $\text{Mn}(\text{als})_2$ the $\text{Mn}-\text{N}_m$ length, 2.004 (3) Å, has the same value, the $\text{Mn}-\text{O}_c$ length, 1.907 (2) Å, is slightly longer, and $\text{Mn}-\text{O}_p$, 1.860 (2) Å, is slightly shorter. The $\text{Mn}-\text{O}_p$ distances in three catechol complexes^{5a,b,c} fall in the range 1.853 (2)–1.922 (3) Å. The structure of an anionic manganese(III) bis complex of the glycine analogue of H_2als is known.¹⁹ The average $\text{Mn}-\text{O}_c$ and $\text{Mn}-\text{O}_p$ distances are ~ 0.1 Å longer than those in $\text{Mn}(\text{als})_2$.

The spectral, magnetic, and electrochemical properties of $\text{Mn}(\text{ans})_2$ and $\text{Mn}(\text{ann})_2$ are closely analogous to those of $\text{Mn}(\text{als})_2$. It is therefore reasonable to assume that they also have

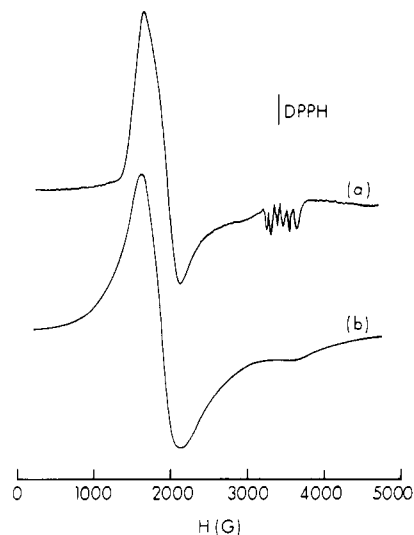


Figure 4. X-Band EPR spectra at 77 K: (a) $\text{Mn}(\text{als})_2$ in dichloromethane-toluene (1:1); (b) $\text{Mn}(\text{ann})_2$ in polycrystalline form.

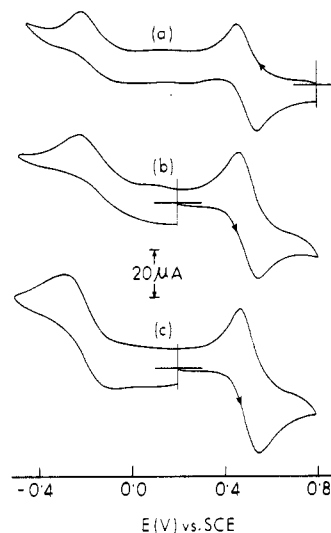


Figure 5. Cyclic voltammograms (scan rate 50 mV s^{-1}) of $\sim 10^{-3}$ M solutions of (a) $\text{Mn}(\text{als})_2$, (b) $\text{KMn}(\text{als})_2 \cdot \text{H}_2\text{O}$, and (c) $\text{KMn}(\text{ans})_2 \cdot \text{H}_2\text{O}$ in methanol (0.1 M TEAP) at a platinum electrode (298 K).

Table IV. Reduction Potentials and Coulometric Data^a in Methanol at 298 K

complex ^b	Mn(IV)–Mn(III)		Mn(III)–Mn(II)
	E_{298}° , V (ΔE_p , mV) ^c	n^d	
$\text{Mn}(\text{als})_2$	0.50 (80)	1.01	–0.22
$\text{Mn}(\text{ans})_2$	0.50 (80)	1.03	–0.28
$\text{Mn}(\text{ann})_2$	0.51 (80)	0.99	–0.29

^a Supporting electrolyte is TEAP (0.1 M); working electrode is platinum; reference electrode is SCE. ^b Because of solubility reasons, data were collected by using $\text{Mn}(\text{als})_2$, $\text{KMn}(\text{als})_2 \cdot \text{H}_2\text{O}$, $\text{KMn}(\text{ans})_2 \cdot \text{H}_2\text{O}$, and $\text{KMn}(\text{ann})_2 \cdot \text{H}_2\text{O}$; the first two compounds gave identical voltammograms. ^c E_{298}° is calculated as the average of anodic (E_{pa}) and cathodic (E_{pc}) peak potentials; $\Delta E_p = E_{pa} - E_{pc}$. ^d Constant-potential coulometric data $n = Q/Q'$, where Q is the observed coulomb count and Q' is the calculated coulomb count for 1e transfer. For $\text{KMnL}_2 \cdot \text{H}_2\text{O}$ complexes oxidations were performed at 0.75 V, and for $\text{Mn}(\text{als})_2$ reduction was done at 0.26 V vs SCE. ^e Cathodic peak potential.

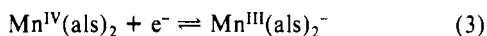
the MnO_4N_2 coordination sphere with meridionally spanning ligands.

D. Magnetism and EPR Spectra. The magnetic moments of the MnL_2 complexes (Table III) correspond to the presence of three unpaired electrons ($3d^3$). Their X-band EPR spectra are shown in Figure 4, and parameters are listed in Table III. In the polycrystalline phase the MnL_2 (298, 77 K) complexes display

- (16) Bag, N.; Lahiri, G. K.; Bhattacharya, S.; Falvello, L. R.; Chakravorty, A. *Inorg. Chem.* **1988**, *27*, 4396–4402.
- (17) The distribution on the basis of ligand is halide (two),¹¹ porphyrin (two),^{9a,c} catechol (three),^{5a-c} salicylaldehyde (one),^{6a} salicylic acid (one),⁷ dithiocarbamate (one),^{3a} and organometallic (one).^{10a}
- (18) The structures of a very small number of polynuclear complexes containing manganese(IV) are also known.^{12a,c-f,h}
- (19) Tamura, H.; Ogawa, K.; Sakurai, T.; Nakahara, A. *Inorg. Chim. Acta* **1984**, *92*, 107–111.

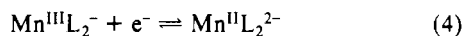
broad to very broad resonances near g values of 2 and 4. Spectra in frozen solution (77 K), which could be obtained only for Mn(als)_2 (for solubility reasons), are better resolved, and the signal near $g = 2$ shows ^{55}Mn hyperfine structure. The average coupling constant is 77 G, which is compatible with the assigned metal oxidation state.²⁰ A much more intense signal devoid of metal hyperfine structure occurs at lower field. The signal is slightly asymmetric and has turnover and crossover points at 1660 G ($g = 4.18$) and 1960 G ($g = 3.54$), respectively.

E. Redox Potentials. In methanolic solution both Mn(als)_2 (initial scan cathodic) and $\text{KMn(als)}_2 \cdot \text{H}_2\text{O}$ (initial scan anodic) display (Figure 5, Table IV) the same cyclic voltammograms with a well-defined one-electron nearly reversible response at ~ 0.5 V vs SCE (eq 3). The two species can be quantitatively inter-



converted by coulometry. Since Mn(als)_2 and Mn(ann)_2 are insoluble (this forms the basis of their electrosynthesis), the couples corresponding to eq 3 were studied with the help of soluble $\text{KMnL}_2 \cdot \text{H}_2\text{O}$ in their cases (Figure 5, Table IV).

A second couple with a cathodic peak near -0.2 V vs SCE is also observed. Here the anodic peak is poorly defined (Figure 5). Current height comparisons suggest that this is also an one-electron process possibly involving the manganese(II) complex (eq 4). However, attempted coulometric reduction leads to



extensive decomposition. The nature of the manganese(II) complex is unclear at present.

Discussion

In a crystal field of strict octahedral symmetry a d^3 ion has ${}^4A_{2g}$ ground state leading to an isotropic resonance at $g \approx 2$.^{11b,20a} Distortion and spin-orbit coupling split the ground quartet into two Kramers doublets separated by $2(D^2 + 3E^2)^{1/2}$, where D and E are respectively axial and rhombic zero-field-splitting parameters. The nature of polycrystalline or glassy-state EPR spectra of distorted d^3 complexes vary widely depending on values of D , E , and the microwave quantum value ($h\nu = 0.31$ cm⁻¹ for X-band).²¹ Simplification occurs under certain limiting conditions.⁴ Of interest here is the situation where the distortion is primarily axial and strong: $D \gg E$ and $2D \gg h\nu$. Two main resonances are expected in this limit: a strong one near $g = 4$ and a weak one near $g = 2$. A good example is $\text{Cr(py)}_4\text{X}_2^+$ ($X = \text{Cl, Br}$).^{21a}

The EPR spectra of MnL_2 along with those of certain other manganese(IV) complexes^{5b,5d,8a,9a} broadly correspond to strong axial distortion. In a rectangular coordinate system with z as the symmetry axis the signals near $g = 4$ and 2 can be identified as $g_{x,y}$ and g_z , respectively.^{9a,21a} The low-field signal of Mn(als)_2 is slightly asymmetric, and it extends unequally above and below the crossover point whose g value is 3.54. This behavior is assigned to unresolved splitting of the $g_{x,y}$ signal due to the presence of a small but significant rhombic component in the ligand field. The EPR spectra of the tetraphenylporphyrin complex $\text{Mn(tpp)}(\text{NCO})_2$ ^{9a} (^{55}Mn structure only on g_z as in Mn(als)_2) and of a pyrazolylborate complex²² described after submission of this work have similar characteristics.

In the water-oxidation complex of photosystem II manganese is present in O- and/or nonporphyrinic N-coordination.¹ Carboxylate and phenolate functions of the amino acid residues could account for O-binding.^{7,8a} The S_2 state of the water-oxidation

Table V. Crystallographic Data for Mn(als)_2

chem formula $\text{C}_{20}\text{H}_{18}\text{N}_2\text{O}_6\text{Mn}$	$Z = 4$
fw 437.3	$T = 23 \pm 1$ °C
space group $C2/c$	$\lambda = 0.71073$ Å
$a = 17.314$ (5) Å	$\rho_{\text{calcd}} = 1.625$ g cm ⁻³
$b = 7.884$ (3) Å	$\mu = 7.50$ cm ⁻¹
$c = 13.104$ (3) Å	transm coeff = 0.7897–0.7148
$\beta = 91.86$ (2)°	$R^a = 0.0438$
$V = 1787.8$ (9) Å ³	$R_w^b = 0.0581$

$$^a R = \sum ||F_o| - |F_c|| / \sum |F_o|. \quad ^b R_w = [\sum w(|F_o| - |F_c|)^2 / \sum w|F_o|^2]^{1/2}; w^{-1} = \sigma^2(|F_o|) + 0.0004|F_o|^2.$$

Table VI. Atomic Coordinates ($\times 10^4$) and Equivalent Isotropic Displacement Coefficients ($\text{Å}^2 \times 10^3$) (with Their Estimated Standard Deviations in Parentheses) for Mn(als)_2 ^a

atom	x	y	z	$U(\text{eq})$
Mn	0	3252 (1)	2500	36 (1)
N(1)	681 (1)	3285 (4)	1292 (2)	40 (1)
O(1)	-607 (1)	1580 (3)	1874 (2)	43 (1)
O(2)	611 (1)	4995 (3)	3131 (2)	44 (1)
O(3)	1656 (1)	6417 (3)	3607 (2)	59 (1)
O(1)	-796 (2)	1511 (4)	884 (2)	38 (1)
C(2)	-303 (2)	2124 (4)	131 (2)	39 (1)
C(3)	-506 (2)	1869 (5)	-908 (2)	48 (1)
C(4)	-1192 (2)	1124 (6)	-1194 (3)	57 (1)
C(5)	-1680 (2)	556 (5)	-452 (3)	57 (1)
C(6)	-1478 (2)	712 (5)	579 (3)	53 (1)
C(7)	441 (2)	2840 (4)	392 (2)	40 (1)
C(8)	1482 (2)	3948 (6)	1372 (3)	67 (1)
C(9)	1799 (2)	4229 (7)	2381 (3)	73 (2)
C(10)	1344 (2)	5324 (5)	3091 (2)	42 (1)

^aEquivalent isotropic U defined as one-third of the trace of the orthogonalized U_{ij} tensor.

complex displays multiline EPR spectra with a strong signal near $g = 4$ devoid of ^{55}Mn structure. The latter signal has been attributed to an approximately axially symmetric mononuclear manganese(IV) center.^{1f} If this is true, the MnL_2 complexes are mimetic of the above center both in terms of coordination environment and EPR spectra.

The formal symmetry of Mn(als)_2 as revealed by structure determination is rhombic (C_2). However, the MnO_4N_2 coordination sphere has a nearly perfect O_4 equator with respect to which the two N atoms are located in virtually ideal trans positions. The Mn–N distance is longer than the average Mn–O distance by more than 0.1 Å. This is significantly larger than the difference in covalent radii of N and O. Thus, the primary distortion of the MnO_4N_2 octahedron is axial elongation along the MnN_2 axis. The EPR spectrum of Mn(als)_2 is in qualitative agreement with this.

The MnL_2 complexes are oxidizing but not sufficiently so to convert water into dioxygen. The manganese(IV)–manganese(III) reduction potentials are known in three other groups of $\text{Mn}^{\text{IV}}\text{O}_4\text{N}_2$ complexes. In a salicylate–pyridine complex an irreversible manganese(IV)–manganese(III) couple is observed with a cathodic peak potential of 0.44 V vs SCE in dimethylformamide.⁷ In hydroxyl-rich salicylaldehydes^{6a,d} and in N -(hydroxyphenyl)-salicylamides^{8b} the reduction potentials lie at negative potentials. We take particular note of the fact that in carboxylate coordinated MnL_2 the potential is ~ 800 mV more positive than those in salicylaldehyde complexes involving alkoxide coordination.^{6a} This qualitatively correlates with the higher base strength of the alkoxide function ($\text{pK} > 13$) compared to the carboxylate function ($\text{pK} \sim 4$).²³ The water-oxidation site of photosystem II must have a high reduction potential. Carboxylate coordination of

- (20) (a) McGarvey, B. R. In *Transition Metal Chemistry*; Carlin, R. L., Ed.; Marcel Dekker: New York, 1966; Vol. 3, p 89. (b) Rasmussen, P. G.; Beem, K. M.; Hornyak, E. J. *J. Chem. Phys.* **1969**, *50*, 3647–3648. (c) Nakadu, M.; Awazu, K.; Ibuki, S.; Miyako, T.; Date, M. *J. Phys. Soc. Jpn.* **1964**, *19*, 781–786.
- (21) (a) Pederson, E.; Toftlund, H. *Inorg. Chem.* **1974**, *13*, 1603–1612. (b) Bradley, D. C.; Copperthwaite, R. G.; Cotton, S. A.; Sales, K. D.; Gibson, J. F. *J. Chem. Soc., Dalton Trans.* **1973**, 191–194. (c) Hempel, J. C.; Morgan, L. O.; Lewis, W. B. *Inorg. Chem.* **1970**, *9*, 2064–2072. (d) Singer, L. S. *J. Chem. Phys.* **1955**, *23*, 379–388.
- (22) Chan, M. K.; Armstrong, W. H. *Inorg. Chem.* **1989**, *28*, 3777–3779.

- (23) A reviewer has suggested that the good reversibility of the couple of eq 3 may be due to the near-octahedral geometry of MnL_2 . In related but distorted (strained) systems the manganese(IV)–manganese(III) couple is quasireversible at best.^{6a} It is argued that the reduction to the manganese(III) level is more facile in MnL_2 than in the strained systems, since the latter would tend to dissociate an arm upon Jahn–Teller elongation of the d^4 ion.

manganese center(s) is a plausible instrument for achieving this end in nature.

Concluding Remarks

The first group of manganese(IV) salicylaldiminates involving carboxylate oxygen binding are described. These have effectively axial MnO_4N_2 coordination. The complexes are biomimetic of photosystem II both in coordination environment and in EPR spectra. However, these are insufficiently oxidizing for oxygen evolution from water. The role of carboxylate coordination in raising the manganese(IV)-manganese(III) reduction potential is specially noted. We have recently demonstrated that amide coordination has the reverse effect.^{8a}

The utility of $X-O^-$ ligands in binding manganese(IV) gains further ground with the present system. Ongoing work concerns use of new $X-O^-$ and other types of ligands for chelating manganese(IV) into structurally characterizable species. The 2-fold purpose is to establish that manganese(IV) is an easily accessible oxidation state and to purposefully modulate manganese redox potentials by varying the coordination environment.

Experimental Section

Materials. $Mn(CH_3CO_2)_2 \cdot 2H_2O$ was prepared as reported.²⁴ Electrochemically pure CH_3OH and tetraethylammonium perchlorate (TEAP) were obtained as before.²⁵ All other chemicals and solvents were of analytical grade and used as obtained.

Physical Measurements. Electronic spectra were recorded with an Hitachi 330 spectrophotometer. X-Band EPR spectra were collected on a Varian E-109C spectrometer fitted with a quartz Dewar flask for low-temperature measurements (liquid dinitrogen, 77 K). DPPH ($g = 2.0037$) was used to calibrate the EPR spectra. Magnetic susceptibilities were measured by using a PAR-155 vibrating-sample magnetometer fitted with a Walker Scientific L 75FBAL magnet. Solution ($\sim 10^{-3}$ M) electrical conductivities were measured with the help of Philips PR 9500 bridge. A Perkin-Elmer 240C elemental analyzer was used to collect microanalytical data (C, H, N). Electrochemical measurements were performed on a PAR Model 370-4 electrochemistry system incorporating the following: Model 174A, polarographic analyzer; Model 175, universal programmer; Model RE 0074, XY recorder; Model 173, potentiostat; Model 179, digital coulometer; Model 377A, cell system. All experiments were done under dry and purified dinitrogen atmosphere at 298 K. A planar Beckman Model 39273 platinum-inlay working electrode, a platinum-wire auxiliary electrode, and an aqueous saturated calomel reference electrode (SCE) were used in the three-electrode measurements. A platinum-wire-gauze working electrode was used in coulometric experiments. All potentials reported in this work are uncorrected for junction contribution.

Preparation of Compounds. *N*-(2-Carboxyphenyl)salicylideneamine, H_2ans . A 2.50-g (0.02-mol) sample of salicylaldehyde and 2.8 g (0.02 mol) of anthranilic acid were taken in 25 mL of absolute ethanol, and the mixture was stirred at room temperature for 1 h. An orange solid precipitated. It was collected by filtration and was purified by recrystallization from ethanol (mp 158 °C). The yield was 4.20 g (85%). Anal. Calcd for $C_{14}H_{11}NO_3$: C, 69.71; H, 4.56; N, 5.81. Found: C, 69.52; H, 4.45; N, 5.64.

Anal. Calcd for H_2als (mp 92 °C) and H_2ann (mp 224 °C) prepared by using the same procedure from appropriate starting materials are as follows: Anal. Calcd for H_2als , $C_{10}H_{11}NO_3$: C, 62.18; H, 5.70; N, 7.25. Found: C, 61.83; H, 5.61; N, 7.10. Calcd for H_2ann , $C_{18}H_{13}NO_3$: C, 74.23; H, 4.47; N, 4.81. Found: C, 73.94; H, 4.23; N, 4.66.

Potassium Bis(*N*-(2-carboxyphenyl)salicylideneaminate)manganate(III) Hydrate, $KMn(ans)_2 \cdot H_2O$. To a methanolic solution (20 mL) of H_2ans (0.55 g, 2.28 mmol) was added $Mn(OAc)_2 \cdot 2H_2O$ (0.30 g, 1.12 mmol). The orange solution immediately became deep brown. To this was added KOH (0.25 g, 4.46 mmol), and the mixture was stirred at room temperature for 2 h. A green solid separated. It was collected by filtration and washed with ice-cold water-acetonitrile mixed solvent. Finally the compound dried under vacuum over P_4O_{10} ; yield 0.62 g (92%). Anal. Calcd for $KMnC_{28}H_{20}N_2O_7$: Mn, 9.31; C, 56.95; H, 3.39; N, 4.75. Found: Mn, 9.20; C, 57.34; H, 3.68; N, 4.78.

$KMn(als)_2 \cdot H_2O$ and $KMn(ann)_2 \cdot H_2O$ were synthesized similarly from H_2als and H_2ann , respectively, as dark and green solids. Anal. Calcd for $KMn(als)_2 \cdot H_2O$, $KMnC_{20}H_{20}N_2O_7$: Mn, 11.12; C, 48.58; H, 4.05; N, 5.67. Found: Mn, 11.33; C, 48.21; H, 3.95; N, 5.46. Calcd for $KMn(ann)_2 \cdot H_2O$, $KMnC_{36}H_{24}N_2O_7$: Mn, 7.96; C, 62.60; H, 3.48; N, 4.06. Found: Mn, 7.84; C, 62.27; H, 3.40; N, 3.80.

Bis(*N*-(2-carboxyethyl)salicylideneaminate)manganese(IV), $Mn(als)_2$. An aqueous solution (25 mL) of $K_2S_2O_8$ (0.20 g, 0.74 mmol) was added to a methanol solution (15 mL) of $KMn(als)_2 \cdot H_2O$ (0.50 g, 1.01 mmol). The mixture was stirred at room temperature for 1/4 h. The color of the solution became green, and the solution was extracted with dichloromethane. Excess hexane was added to this green dichloromethane solution, and a dark solid separated. It was collected by filtration and dried under vacuum; yield 0.35 g (79%). Anal. Calcd for $MnC_{20}H_{18}N_2O_6$: Mn, 12.57; C, 54.93; H, 4.12; N, 6.41. Found: Mn, 12.40; C, 54.70; H, 4.13; N, 6.23.

$Mn(ans)_2$ and $Mn(ann)_2$ were similarly synthesized in ~85% yield. In these cases the compounds precipitated during oxidation due to their poor solubility and dichloromethane extraction was not necessary. The precipitates were collected by filtration, washed with water, and dried under vacuum over P_4O_{10} . Anal. Calcd for $Mn(ans)_2$, $MnC_{28}H_{18}N_2O_6$: Mn, 10.31; C, 63.05; H, 3.38; N, 5.25. Found: Mn, 10.12; C, 62.78; H, 3.33; N, 5.11. Calcd for $Mn(ann)_2$, $MnC_{36}H_{22}N_2O_6$: Mn, 8.68; C, 68.25; H, 3.48; N, 4.42. Found: Mn, 8.49; C, 68.12; H, 3.50; N, 4.25.

In the preparation of $Mn(als)_2$ silver perchlorate can be used instead of $K_2S_2O_8$ as a very efficient oxidant. In the cases of $Mn(ans)_2$ and $Mn(ann)_2$ only $K_2S_2O_8$ was used to avoid contamination by metallic silver as they precipitate during oxidation.

Electrosynthesis of Bis(*N*-(2-carboxyphenyl)salicylideneaminate)manganese(IV), $Mn(ans)_2$. A solution of 100 mg (0.17 mmol) of $KMn(ans)_2 \cdot H_2O$ in 30 mL of dry methanol (0.1 M TEAP) was oxidized coulometrically at a constant potential of 0.75 V vs SCE in nitrogen atmosphere. As oxidation proceeds, the color of the solution turns green (from initial brown) and then gradually fades. A dark solid deposited in the coulometric cell. After exhaustive electrolysis the solid was collected by filtration, washed thoroughly with methanol, and finally dried under vacuum; yield 80 mg (89%).

The $Mn(ann)_2$ complex can be prepared similarly in ~90% yield from $KMn(ann)_2 \cdot H_2O$.

X-ray Structure Determination. Single crystals of $Mn(als)_2$ were grown by slow evaporation of a dichloromethane-methanol (1:1) solution of the compound. A dark prismatic crystal was mounted in a thin-walled glass capillary. Data collection was performed on a Nicolet R3m/V automated diffractometer using graphite-monochromated Mo $K\alpha$ radiation ($\lambda = 0.71073 \text{ \AA}$). Significant crystal data and data collection parameters are listed in Table V. The unit cell parameters were determined by least-squares fit of 20 reflections (selected from a rotation photograph) having 2θ values in the range 5–25°. Lattice dimensions and the Laue group were checked by axial photography. Systematic absences led to the identification of the space group as Cc or $C2/c$. The structure was successfully solved in the latter space group.

During data collection the parameters kept fixed were as follows: an ω range of 1.80°; variable scan speed between 3.0 and 25.0° min^{-1} ; ratio of background/scan time 0.5. Three check reflections were measured after every 97 reflections during data collection to monitor the crystal stability. No significant intensity reduction was observed in the 35.5 h of exposure to X-rays. All data were corrected for decay (decay correction range on I was 0.9906–1.0409) and Lorentz-polarization effects. An empirical absorption correction was done on the basis of azimuthal scans²⁶ of eight reflections with χ near 287° and 2θ in the range 23–44°.

All calculations for data reduction, structure solution, and refinement were done on a MicroVAX II computer with the programs of SHELXTL-PLUS.²⁷ The position of the unique manganese atom was determined from a Patterson map. The remainder of the structure (except hydrogen atoms) emerged from a difference Fourier map. The model was then refined by full-matrix least-squares procedures. All non-hydrogen atoms were made anisotropic. Hydrogen atoms of the benzene rings were located in a difference map and were refined isotropically with fixed thermal parameters. Methylene hydrogen atoms were included in calculated positions by using a riding model. The final refinement involved a scale factor, 15 anisotropic non-hydrogen atoms and 9 isotropic hydrogen atoms. The final, convergent refinement gave residuals as summarized in Table V. No correlations were observed in the final refinement, and the highest difference Fourier peak was 0.22 $e/\text{\AA}^3$.

(24) Brauer, G., Ed. *Handbook of Preparative Inorganic Chemistry*; Academic Press: New York, 1965; Vol. 2, pp 1469–1470.

(25) Datta, D.; Mascharak, P. K.; Chakravorty, A. *Inorg. Chem.* **1981**, *20*, 1673–1679.

(26) North, A. C. T.; Philips, D. C.; Mathews, F. S. *Acta Crystallogr., Sect. A* **1968**, *24*, 351–359.

(27) Sheldrick, G. M. *SHELXTL-Plus 88, Structure Determination Software Programs*; Nicolet Instrument Corp.: 5225-2 Verona Road, Madison, WI 53711, 1988.

Atomic coordinates and isotropic equivalent thermal parameters are collected in Table VI.

Acknowledgment. We are very thankful to the Department of Science and Technology, New Delhi, for establishing a National Single Crystal Diffractometer Facility at the Department of Inorganic Chemistry, Indian Association for the Cultivation of Science. Financial support received from the Council of Scientific

and Industrial Research is also acknowledged. Comments of reviewers were helpful at the revision stage.

Supplementary Material Available: Listings of anisotropic thermal parameters (Table VII), complete bond distances (Table VIII) and angles (Table IX), and hydrogen atom positional parameters (Table X) and a structure determination summary (Table XI) (5 pages); a listing of observed and calculated structure factors (8 pages). Ordering information is given on any current masthead page.

Contribution from The Squibb Institute for Medical Research,
P.O. Box 191, New Brunswick, New Jersey 08903

Neutral, Seven-Coordinate Dioxime Complexes of Technetium(III): Synthesis and Characterization

Karen E. Linder, Mary F. Malley, Jack Z. Gougoutas, Steve E. Unger,[†] and Adrian D. Nunn*

Received February 8, 1989

The tin-capped complexes $^{99}\text{Tc}(\text{oxime})_3(\mu\text{-OH})\text{SnCl}_3$ [oxime = dimethylglyoxime (DMG) or cyclohexanedione dioxime (CDO)] can be prepared by the reduction of NH_4TcO_4 with 2 equiv of SnCl_2 in the presence of dioxime and HCl. These tin-capped complexes can be readily converted into a new class of uncapped Tc-dioxime compounds, $\text{TcCl}(\text{oxime})_3$, by treatment with HCl. This reaction is reversible. Both the tin-capped and uncapped tris(dioxime) complexes can be converted to the previously reported boron-capped Tc-dioxime complexes $\text{TcCl}(\text{oxime})_3\text{BR}$ (R = alkyl, OH) by reaction with boronic acids or with boric acid at low pH. All of these complexes [$\text{Tc}(\text{oxime})_3(\mu\text{-OH})\text{SnCl}_3$, $\text{TcCl}(\text{oxime})_3$, and $\text{TcCl}(\text{oxime})_3\text{BR}$] appear to be neutral, seven-coordinate compounds of technetium(III). They have been characterized by elemental analysis, ^1H NMR and UV/visible spectroscopy, conductivity, and fast atom bombardment mass spectrometry. The synthesis, characterization, and reactivity of these compounds is discussed. The X-ray crystal structure analysis of $\text{TcCl}(\text{DMG})_3$ and an abbreviated structure report on $\text{TcCl}(\text{DMG})_3\text{MeB}$ are described. Crystal data for $\text{TcCl}(\text{DMG})_3$: $a = 9.617$ (1) Å, $b = 12.135$ (3) Å, $c = 9.244$ (2) Å, $\alpha = 110.24$ (2)°, $\beta = 92.36$ (2)°, $\gamma = 88.92$ (2)°, space group = $P\bar{1}$, $Z = 2$. Final $R = 0.041$; $R_w = 0.047$. Data for $\text{TcCl}(\text{DMG})_3\text{MeB}$: $a = 20.290$ (3) Å, $b = 14.468$ (2) Å, $c = 16.404$ (3) Å, $\beta = 124.65$ (1)°, space group = $C2/c$, $Z = 8$. Final $R = 0.039$; $R_w = 0.044$.

Introduction

We have recently prepared¹ a large number of neutral, seven-coordinate technetium(III) dioxime complexes, $\text{TcX}(\text{oxime})_3\text{BR}$ (X = halogen, R = alkyl, OH), which are capped at one end through three dioxime oxygens by a tetravalent boron atom. This BATO (boronic acid adducts of technetium dioximes) class of complexes (Figure 1) can be prepared by SnCl_2 reduction of $^{99}\text{TcO}_4^-$ in the presence of vicinal dioximes and a boronic acid. Our interest in these complexes stems from the fact that several of them exhibit myocardial² or brain³ uptake, when prepared with the short-lived, γ -emitting nuclide, ^{99m}Tc . Two compounds in this class, $\text{TcCl}(\text{CDO})_3\text{MeB}$ and $\text{TcCl}(\text{DMG})_3(2\text{MP})$, are currently in clinical trials as agents for imaging heart and brain perfusion. (CDO = cyclohexanedione dioxime, DMG = dimethylglyoxime, MeB = methylboron, 2MP = (2-methyl-1-propyl)boron.)

These BATO complexes form via template synthesis.⁴ To better understand how these complexes are formed from $^{99}\text{TcO}_4^-$, we have examined this reaction in detail. We report here the synthesis and characterization of two dioxime-containing intermediates that are precursors to the BATO compounds, $\text{Tc}(\text{oxime})_3(\mu\text{-OH})\text{SnCl}_3$ and $\text{TcCl}(\text{oxime})_3$ (oxime = DMG, CDO).

The complex $\text{Tc}(\text{DMG})_3(\mu\text{-OH})\text{SnCl}_3$ was first prepared by Deutsch et al.,⁵ using a modification of an analytical procedure⁶ for the detection of technetium. Addition of excess chlorostannic acid to an acidic mixture of TcO_4^- and DMG yields a deep green solution. Deutsch et al. allowed this green solution to go to near dryness over several weeks and isolated yellow crystals from the reaction mixture in low yield. The preparation was not reproducible; therefore, only the X-ray crystal structure analysis⁵ of the complex was reported. Libson⁷ later found that H_2O_2 could oxidize the green precursor to the desired yellow complex in solution and reported the UV/visible spectra of the DMG complex

Table I. Crystallographic Parameters for $\text{TcCl}(\text{DMG})_3$

formula	$\text{TcCl}_{12}\text{H}_{22}\text{N}_6\text{ClO}_6 \cdot 0.5\text{CH}_2\text{Cl}_2$
fw	523.27
space group	$P\bar{1}$
a , Å	9.617 (1)
b , Å	12.135 (3)
c , Å	9.244 (2)
α , deg	110.24 (2)
β , deg	92.36 (2)
γ , deg	88.92 (2)
V , Å ³	1011.3 (8)
Z	2
D_{calc} , g/cm ³	1.72
D_{obs} (floatation), g/cm ³	1.74
cryst size, mm	$0.25 \times 0.15 \times 0.25$
μ , cm ⁻¹	10.0
transm factor	0.87-1.00
scan method	$\theta-2\theta$
scan range (2θ), deg	0-50
no. of reflns measd	4999
no. of indep reflns	4672
no. of data with $F_o^2 \geq 3\sigma$	3350
no. of refined variables	253
R	0.041
R_w	0.047

and its CDO analogue. We have developed an improved synthesis of these yellow tin-capped compounds and have found them to

- (1) (a) Treher, E. N.; Gougoutas, J.; Malley, M.; Nunn, A. D.; Unger, S. E. *J. Labelled Compd. Radiopharm.* **1986**, *23*, 1118. (b) Unger, S. E.; McCormick, T. J.; Treher, E. N.; Nunn, A. D. *Anal. Chem.* **1987**, *59*, 1145. (c) Treher, E. N.; Francesconi, L. C.; Gougoutas, J. Z.; Malley, M. F.; Nunn, A. D. *Inorg. Chem.* **1989**, *28*, 3411.
- (2) (a) Coleman, R. E.; Maturi, M.; Nunn, A. D.; Eckelman, W.; Juri, P. N.; Cobb, F. R. *J. Nucl. Med.* **1986**, *27*, 893. (b) Narra, R. K.; Feld, T.; Wedeking, P.; Nunn, A. D. In *Nuclear Medicine: Clinical Demands on Nuclear Chemistry*; Schmidt, H. A. E., Emrich, D., Eds.; F. K. Schattauer Verlag: New York, 1987; p 489. (c) Seldin, D. W.; Johnson, L. L.; Blood, D. K.; Muschel, M. J.; Smith, K. F.; Wall, R. M.; Cannon, P. J. *J. Nucl. Med.* **1989**, *30*, 312.

* Author to whom correspondence should be addressed.

[†] Present address: Department of Drug Metabolism, Glaxo Inc., Research Triangle Park, NC 27709.